Cell Research (2016) 26:728-742.

www.nature.com/cr

ORIGINAL ARTICLE

Loss of MeCP2 in cholinergic neurons causes part of RTT-like phenotypes via α7 receptor in hippocampus

Ying Zhang[1, *], Shu-Xia Cao[1, *], Peng Sun[1], Hai-Yang He[1], Ci-Hang Yang[1], Xiao-Juan Chen[1], Chen-Jie Shen[1], Xiao-Dong Wang[1], Zhong Chen[1], Darwin K Berg[2], Shumin Duan[1, 3], Xiao-Ming Li[1, 3]

[1]Department of Neurobiology, Institute of Neuroscience, Key Laboratory of Medical Neurobiology of the Ministry of Health of China, Collaborative Innovation Center for Brain Science, Zhejiang University School of Medicine, Hangzhou, Zhejiang 310058, China; [2]Neurobiology Section, Division of Biological Sciences and Center for Neural Circuits and Behavior, University of California, San Diego, La Jolla, CA 92093-0357, USA; [3]Soft Matter Research Center, Zhejiang University, Hangzhou, Zhejiang, China

Mutations in the X-linked *MECP2* gene cause Rett syndrome (RTT), an autism spectrum disorder characterized by impaired social interactions, motor abnormalities, cognitive defects and a high risk of epilepsy. Here, we showed that conditional deletion of *Mecp2* in cholinergic neurons caused part of RTT-like phenotypes, which could be rescued by re-expressing *Mecp2* in the basal forebrain (BF) cholinergic neurons rather than in the caudate putamen of conditional knockout (*Chat-Mecp2*$^{-/y}$) mice. We found that choline acetyltransferase expression was decreased in the BF and that α7 nicotine acetylcholine receptor signaling was strongly impaired in the hippocampus of *Chat-Mecp2*$^{-/y}$ mice, which is sufficient to produce neuronal hyperexcitation and increase seizure susceptibility. Application of PNU282987 or nicotine in the hippocampus rescued these phenotypes in *Chat-Mecp2*$^{-/y}$ mice. Taken together, our findings suggest that MeCP2 is critical for normal function of cholinergic neurons and dysfunction of cholinergic neurons can contribute to numerous neuropsychiatric phenotypes.

***Keywords*:** MeCP2; cholinergic system; Rett syndrome; RTT-like phenotypes

Cell Research (2016) **26**:728-742. doi:10.1038/cr.2016.48; published online 22 April 2016

Introduction

Rett syndrome (RTT) [1, 2] is an autism spectrum disorder that affects nearly 1 in 10 000 females [3]. Patients with RTT exhibit a broad range of phenotypes including impaired social behaviors, cognitive defects and motor abnormalities [4, 5]. Clinical studies have shown that nearly 80% of RTT patients suffer recurrent seizures [6]. Furthermore, nearly 70% of RTT patients show patterns of anxiety and over 20% experience "continual or inappropriate laughter", which are supportive criteria for atypical RTT [4-7]. Currently, however, there is no treatment available for RTT due to its specific neurodevelopmental disorders. Thus, understanding the occurrence of various RTT phenotypes is necessary and urgent for developing effective treatments.

Mutations in the X-linked gene encoding the transcriptional regulator MeCP2 are found in more than 95% of classic RTT patients [8, 9]. Mice lacking functional MeCP2 recapitulate major features of RTT [10-12]. Moreover, increased expression of MeCP2 also causes heightened anxiety and autism-like behavior in *Mecp2*-TG1 mice [13]. Despite the pronounced neurological phenotypes in RTT, both *Mecp2*-null mice and RTT patients show normal gross brain structure without obvious neuronal loss, implicating the involvement of neural circuits in the development of RTT phenotypes [14]. Deletion of *Mecp2* from different neuronal types in various brain regions can produce different phenotypes of RTT [15-20]. Subsequent reactivation of *Mecp2* in *Mecp2*-deficient mice also substantially improves behavioral and cellular deficits, suggesting that impaired circuitry in a *Mecp2*-deficient brain can be restored [21-23]. In addition, recent studies have demonstrated that treatment with clenbuterol, an agonist for adrenergic receptors,

*These two authors contributed equally to this work.
Correspondence: Xiao-Ming Li
Tel/Fax: +86-571-8820-8757
E-mail: lixm@zju.edu.cn
Received 21 November 2015; revised 3 February 2016; accepted 17 February 2016; published online 22 April 2016

improves survival and ameliorates diverse phenotypes in *Mecp2* mutant mice [24]. However, carefully-controlled studies are required due to the serious side effects of clenbuterol on humans, suggesting that safer and more effective medication targets are needed for RTT treatment.

Cholinergic signaling in the hippocampus is critical for the etiology of mood disorders and cognitive deficits [25, 26]. Mutations in specific nicotinic receptors can even cause a genetically transmissible form of epilepsy [27]. Moreover, decreases in cholinergic markers have been correlated with clinical severity in RTT patients [28, 29]. The link between cholinergic systems and specific RTT phenotypes led us to hypothesize that dysfunction in cholinergic neurons might be involved in RTT.

In this study, we explored the consequences of *Mecp2* loss from cholinergic neurons and the underlying mechanisms. *Chat-Mecp2*$^{-/y}$ mice showed behavioral deficits, including impaired social interaction, anxiolytic behaviors and seizure penetrance. We focused on basal forebrain (BF) cholinergic neurons because delayed reactivation of *Mecp2* in the BF rather than in the caudate putamen (CPu) rescued the phenotypes seen in *Chat-Mecp2*$^{-/y}$ mice. We reveal that decrease of choline acetyltransferase (ChAT) expression in the BF and impairment of α7 nicotinic acetylcholine receptor (nAChR) signaling in the hippocampus of *Chat-Mecp2*$^{-/y}$ mice lead to neuronal hyperexcitation and increased seizure susceptibility. In addition, application of PNU282987 or nicotine rescued impaired social interaction and anxiolytic behaviors in *Chat-Mecp2*$^{-/y}$ mice.

Results

Selective deletion of MeCP2 in cholinergic neurons led to part of RTT-like phenotypes

We removed *Mecp2* from cholinergic neurons by breeding mice carrying a *Mecp2* allele flanked by *loxp* sites (*Mecp2*$^{flox/-}$) [30] with *Cre* transgenic (*Chat-IRES-Cre*) mice (Supplementary information, Figure S1A). To determine *Mecp2* deletion in cholinergic neurons, we stained BF sections with MeCP2 and ChAT, a marker for cholinergic neurons (Figure 1A). In control littermates, MeCP2 was detected in 95% of cholinergic neurons. In BF sections of *Chat-Mecp2*$^{-/y}$ mice, however, MeCP2 immunoreactivity was abolished from nearly 85% of cholinergic neurons (Figure 1B). These results demonstrated the successful deletion of *Mecp2* from cholinergic neurons with the Cre-LoxP system.

To screen for the presence of RTT-like phenotypes, we performed a battery of behavior tests in *Chat-Mecp2*$^{-/y}$ mice and male littermate controls: wild type (WT), *Chat-IRES-Cre* and *Mecp2*$^{flox/y}$ (with constitutive 50% reduction of MeCP2 levels). First, *Chat-Mecp2*$^{-/y}$ mice showed normal locomotor activity, as demonstrated by a similar total distance traveled in the open field tests to the control mice (Supplementary information, Figure S1B). However, the center-to-total distance ratio showed an increasing trend (Supplementary information, Figure S1C), indicating decreased anxiety-like behavior in *Chat-Mecp2*$^{-/y}$ mice. We performed the elevated plus-maze (EPM) test and found that *Chat-Mecp2*$^{-/y}$ mice spent more time and traveled greater distances in exploring the open arms compared with the control mice (Figure 1C-1E). To confirm this result, several other anxiety-related experiments were performed. In the light-dark (LD) box test, *Chat-Mecp2*$^{-/y}$ mice spent more time in the lit compartment compared with *Chat-IRES-Cre* mice (Supplementary information, Figure S1F). In the zero-maze test for anxiety-like behavior, both the number of entries and time spent in the lit compartment were significantly increased in *Chat-Mecp2*$^{-/y}$ mice (Supplementary information, Figure S1G and S1H). In the tail suspension and forced swim tests, conditional knockout of *Mecp2* in cholinergic systems resulted in decreased immobility time (Figure 1F and 1G). All tests indicated that *Chat-Mecp2*$^{-/y}$ mice showed decreased anxiety- and depression-like behaviors compared with the control mice.

We next performed behavioral tests to assess deficits in social interaction, a prominent symptom of RTT. The three-chamber experiment showed that *Chat-Mecp2*$^{-/y}$ mice had profound deficits in social memory. Both *Chat-Mecp2*$^{-/y}$ and control mice showed no preference for the right or left chamber during the habituation period (Supplementary information, Figure S1I). When we put a stranger mouse in one chamber, both *Chat-Mecp2*$^{-/y}$ and control mice spent more time in the mouse-containing chamber than in the empty chamber (Supplementary information, Figure S1J). They interacted with the stranger mouse rather than explored the empty cage (Figure 1H). When a second stranger mouse was placed in the unoccupied side of chamber to assess discrimination between an unfamiliar and familiar mouse, the control mice showed strong preference for the new mouse, but *Chat-Mecp2*$^{-/y}$ mice did not (Supplementary information, Figure S1K and S1I). We also observed social deficits in *Chat-Mecp2*$^{-/y}$ mice in the open field social interaction test, which examines autism-related behavioral deficits. *Chat-Mecp2*$^{-/y}$ mice interacted significantly less with a stranger mouse in the open field arena compared with the control mice (Supplementary information, Figure S1L). Impairment in social interaction also made them poor nest builders (Supplementary information, Figure S1M). Overall, these behavioral findings suggest that condition-

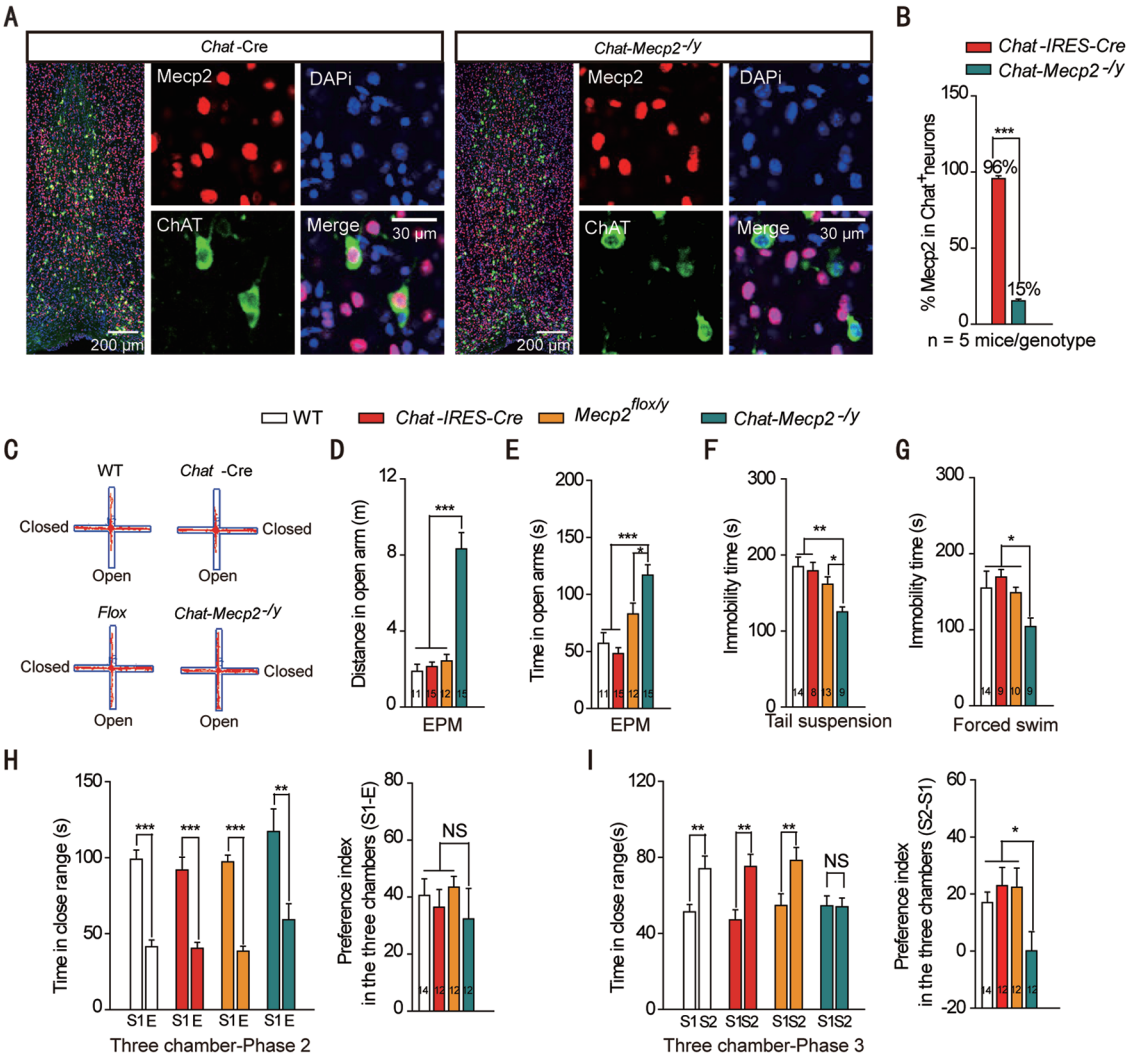

Figure 1 *Chat-Mecp2*$^{-/y}$ mice lost MeCP2 in cholinergic neurons and developed part of RTT-like phenotypes. **(A)** Fluorescence images showing BF sections stained for the nucleus (DAPI), MeCP2 and ChAT. **(B)** Percentage of MeCP2 immunostaining cells in BF cholinergic neurons in *Chat-IRES-Cre* and *Chat-Mecp2*$^{-/y}$ mice (two-sided *t*-test). **(C-E)** Anxiety-related behavior examined by the elevated plus-maze. Data are distance and time that *Chat-IRES-Cre* and *Chat-Mecp2*$^{-/y}$ mice spent in the open arms of the EPM. *P*-values were calculated by one-way ANOVA with Newman-Keuls Multiple Comparison. **(F**, **G)** Depression-related behavior measured by the immobility time that *Chat-IRES-Cre* and *Chat-Mecp2*$^{-/y}$ mice displayed in the tail suspension and forced swim tests. *P*-values were calculated by one-way ANOVA with T Newman-Keuls Multiple Comparison. **(H**, **I)** Social behavior examined in the three-chamber test. **(H)** Left: In the second phase of the three-chamber test, mice of each genotype spent more time on interacting with the stranger mouse than the empty cage. *P*-values were calculated by two-sided *t*-test. Right: Data are ratios of interaction time with a stranger mouse to interaction time with an empty cage. One-way ANOVA with Newman-Keuls Multiple Comparison was used. **(I)** Left, In the third phase, control mice spent more time on interacting with the unfamiliar stranger, and *Chat-Mecp2*$^{-/y}$ mice had no preference for either cage. *P*-values were calculated by two-sided *t*-test. Right: Data are ratios of interaction time with a stranger mouse to interaction time with a familiar mouse. One-way ANOVA with Newman-Keuls Multiple Comparison was used. Error bars are means ± SEM. **P* < 0.05, ***P* < 0.01, ****P* < 0.001.

al deletion of *Mecp2* from cholinergic neurons resulted in aberrant social interaction and social memory.

To determine whether MeCP2 deficiency in cholinergic neurons impaired sensorimotor arousal and gating, which are absent in RTT but typical for schizophrenia, we examined the percentage of pre-pulse inhibition. *Chat-Mecp2*$^{-/y}$ mice showed acoustic startle responses similar to the control mice, revealing that MeCP2 in cho-

linergic systems is not required for sensorimotor gating (Supplementary information, Figure S1N). To determine whether MeCP2 deficiency in cholinergic neurons impaired hippocampal learning and memory, we evaluated *Chat-Mecp2*$^{-/y}$ mice in the Morris water maze paradigm. *Chat-Mecp2*$^{-/y}$ mice showed a similar learning rate during training and spent a similar percentage of time in the target quadrant during the probe test to the control mice (Supplementary information, Figure S1O and Figure S1P). These results indicate that conditional deletion of *Mecp2* from cholinergic systems led to part of RTT-like phenotypes.

Reactivation of Mecp2 in BF but not CPu cholinergic neurons improved phenotypic severity in Chat-Mecp2$^{-/y}$ *mice*

To determine the population of cholinergic neurons involved in RTT phenotypes, we injected the AAV-FLEX-Mecp2-GFP (AAV8/Mecp2) vector into the BF of *Chat-Mecp2*$^{-/y}$ mice to specifically re-express *Mecp2* in the BF cholinergic neurons (Supplementary information, Figure S2A). Immunohistochemical fluorescence analysis of green fluorescent protein (GFP) showed successful vector delivery to the BF (Figure 2A). To confirm the recombination efficiency of the AAV8/Mecp2 virus, we employed dual-label immunohistochemistry and quantified the reactivation efficiency of *Mecp2* in *Chat-Mecp2*$^{-/y}$-AAV8/Mecp2 mice (Supplementary information, Figure S2B-S2D). The results revealed that, within the BF, 87.23% ± 2.3% of GFP-labeled neurons stained positively for

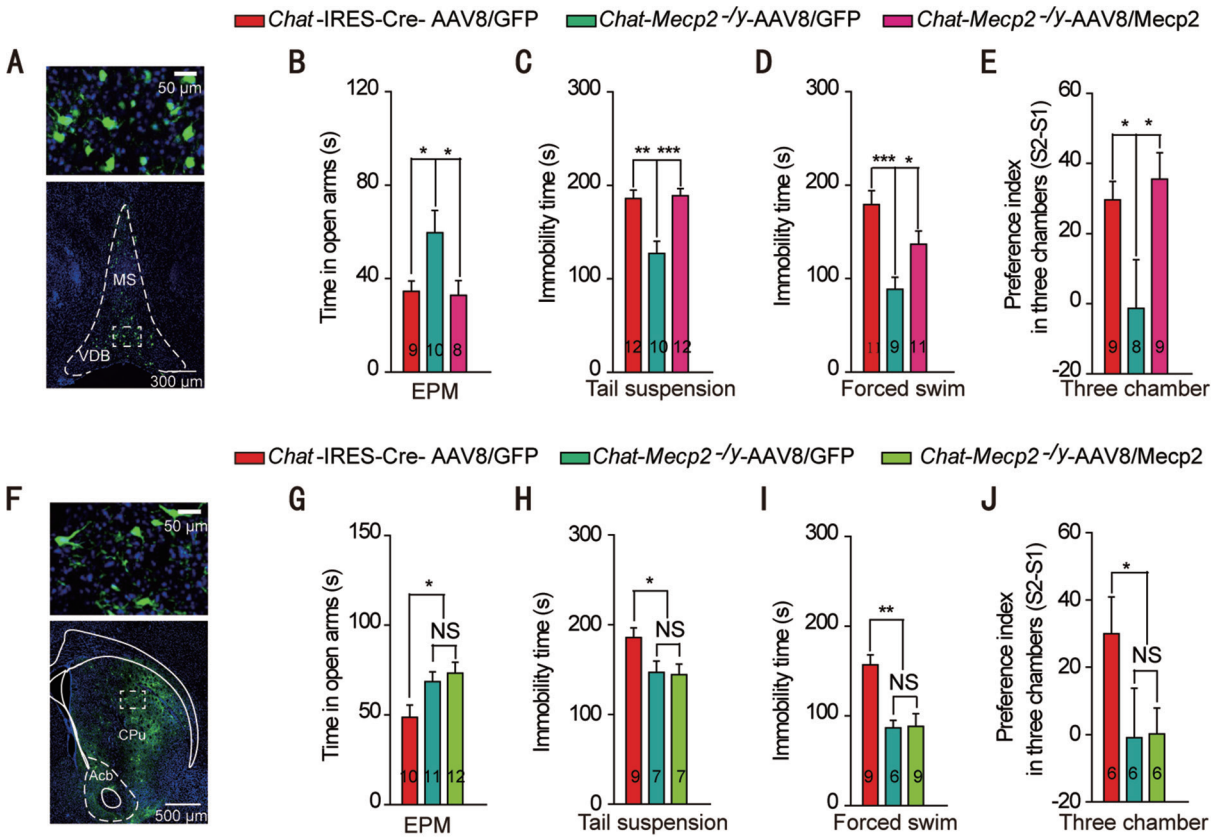

Figure 2 Re-expression of *Mecp2* in BF rather than CPu cholinergic neurons rescued behavioral deficits manifested in *Chat-Mecp2*$^{-/y}$ mice. **(A)** Immunohistochemical analysis showing the distribution of AAV8/Mecp2 in the BF of *Chat-Mecp2*$^{-/y}$ mouse brains 3 weeks after microinjection. **(B)** Anxiety-related behavior measured by the time in the open arms of the EPM. **(C, D)** Depression-related behavior measured by the immobility time that *Chat-IRES-Cre* and *Chat-Mecp2*$^{-/y}$ mice displayed in the tail suspension and forced swim tests. **(E)** Social behavior measured as the ratio of interaction time with a stranger mouse to interaction time with a familiar mouse in the three-chamber test. **(F)** Immunohistochemical analysis showing the distribution of AAV8/Mecp2 in the CPu of *Chat-Mecp2*$^{-/y}$ mouse brains 3 weeks after microinjection. **(G-J)** EPM, tail suspension, forced swim and three-chamber tests performed 3 weeks after injection of the AAV8/Mecp2 virus into the CPu. Error bars are means ± SEM. *P*-values were calculated by two-way ANOVA (genotype × trial) with Bonferroni's *post hoc* comparison. $^{*}P < 0.05$, $^{**}P < 0.01$, $^{***}P < 0.001$.

ChAT and 56.7% ± 5.0% of ChAT-positive neurons were infected with the FLEX virus. Among the infected cholinergic neurons, 46.8% ± 2.0% effectively expressed MeCP2. Consistent with the behavioral findings in Figure 1, AAV8/GFP-injected *Chat-Mecp2*$^{-/y}$ mice showed decreased anxiety- and depression-like behavior compared with AAV8/GFP-injected *Chat-IRES-Cre* mice. However, microinjection of the AAV8/Mecp2 vector into the BF rescued the altered anxiety-related behavior of the *Chat-Mecp2*$^{-/y}$ mice (Figure 2B-2D). To test the effect of regional *Mecp2* re-expression on social behavior, we performed three-chamber tests with the same groups of mice. Data were measured as the ratios of interaction time with a stranger mouse to interaction time with a familiar mouse. *Mecp2* re-expression in the BF cholinergic neurons completely rescued impaired social memory (Figure 2E). In contrast, *Mecp2* re-expression in the CPu cholinergic neurons had no effect on anxiety-related behavior or social behavior in *Chat-Mecp2*$^{-/y}$ mice (Figure 2F-2J). Taken together, these data indicate that MeCP2 in the BF rather than in the CPu cholinergic neurons was specifically involved in the behavioral deficits seen in *Chat-Mecp2*$^{-/y}$ mice.

Deficit in the α7 nAChR signaling pathway from BF cholinergic neurons to the hippocampus in Chat-Mecp2$^{-/y}$ *mice*

To gain insights into the mechanisms by which BF cholinergic neurons promoted RTT phenotypes, we first measured the expression levels of ChAT related to the synthesis of ACh and found that it was downregulated in the BF of *Chat-Mecp2*$^{-/y}$ mice (Figure 3A). However, the GAD65 protein involved in the synthesis of GABA exhibited no significant change. *Chat-IRES-Cre* and *Chat-Mecp2*$^{-/y}$ mice were crossed with Ai9 mice to specifically label cholinergic neurons with tdTomato. Further identification of cholinergic neurons by measuring their membrane properties and firing patterns was based on their distinctive characteristics (Supplementary information, Figure S3C). *Chat-Mecp2*$^{-/y}$ mice showed decreased spontaneous firing frequency compared with *Chat-IRES-Cre* mice (Figure 3B). To exclude the possible influence of constitutive reduction of MeCP2 on *Chat-Mecp2*$^{-/y}$ mice, *Mecp2*$^{flox/y}$ mice were also used as control mice (Supplementary information, Figure S3A and S3B). It has been reported that the hippocampus is the main target for the projection of BF cholinergic neurons [32]. To confirm this, we injected the AAV8/GFP vector into the BF of *Chat-IRES-Cre* mice and detected highly positive signaling in the hippocampal area (Figure 4A). In addition, chronic ACh or nicotine exposure can regulate the response of nAChRs in an activity-dependent manner [33, 34]. Accordingly, we assessed the levels of α7 nAChRs in the hippocampus by western blot analysis and found a significant reduction in the *Chat-Mecp2*$^{-/y}$ mice compared with that in the control mice (Figure 4B). However, the level of gephyrin, a marker for GABAergic synapses, was unchanged (Figure 4B). Ultrastructural analysis suggests that α7 nAChRs are concentrated both presynaptically and postsynaptically at almost all synapses in the CA1 of the hippocampus [35]. However, GABAergic interneurons are much more likely to display detectable levels of 7 nAChRs than GABA-negative neurons [35]. Since parvalbumin (PV)-positive interneurons are the

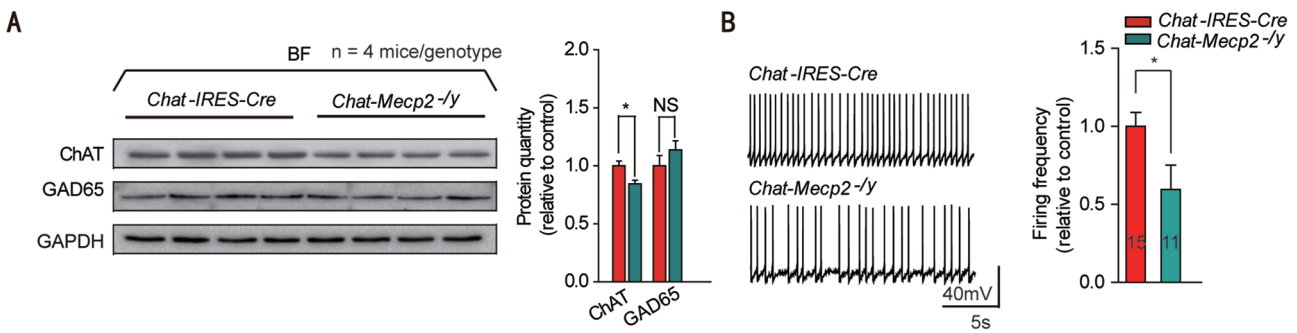

Figure 3 Protein analysis of the BF identified decreased expression of ChAT in *Chat-Mecp2*$^{-/y}$ mice and reduced spontaneous firing of BF cholinergic neurons compared with *Chat-IRES-Cre* mice. **(A)** Left: Immunoblotting of ChAT and GAD65 in BF extracts prepared from *Chat-IRES-Cre* and *Chat-Mecp2*$^{-/y}$ mice. Each lane was loaded with 40 μg of protein with GAPDH as the loading control. Protein levels of *Chat-Mecp2*$^{-/y}$ mice were normalized to the corresponding ones of *Chat-IRES-Cre* mice. Right: Quantification of ChAT and GAD65 proteins in *Chat-IRES-Cre* and *Chat-Mecp2*$^{-/y}$ mice. **(B)** Left: Representative spontaneous firing recordings from BF cholinergic neurons in *Chat-IRES-Cre* and *Chat-Mecp2*$^{-/y}$ mice. Right: Quantification of the firing frequency from BF cholinergic neurons in *Chat-Mecp2*$^{-/y}$ mice normalized by that in *Chat-IRES-Cre* mice. Error bars are means ± SEM. *P*-values were calculated by two-sided *t*-test. **P* < 0.05, ***P* < 0.01, ****P* < 0.001.

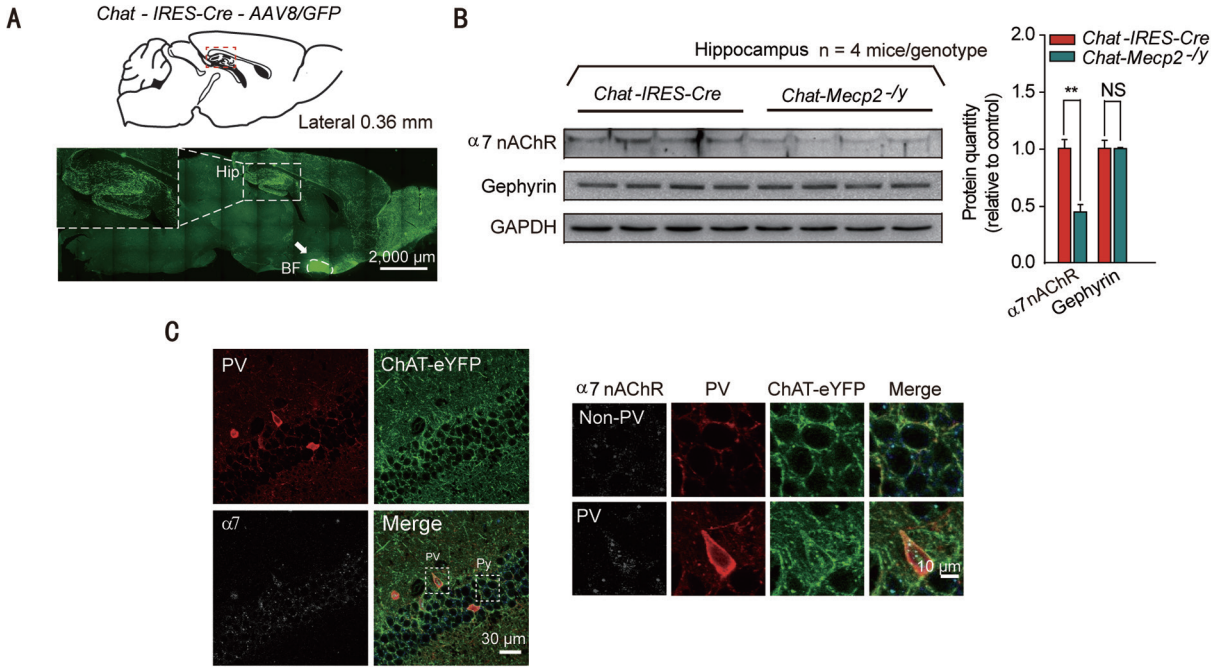

Figure 4 Deficit in α7-nAChR signaling in the hippocampus of *Chat-Mecp2*$^{-/y}$ mice. **(A)** Fluorescence images showing the projection pattern of BF cholinergic neurons labeled by the AAV8/GFP vector in *Chat-IRES-Cre* mice. Arrows, injection site. **(B)** Left: Immunoblotting of α7 nAChR and gephyrin in hippocampal extracts prepared from *Chat-IRES-Cre* and *Chat-Mecp2*$^{-/y}$ mice. Each lane was loaded with 40 μg of protein with GAPDH as the loading control. Protein levels of *Chat-Mecp2*$^{-/y}$ mice were normalized to the corresponding ones of *Chat-IRES-Cre* mice. Right: Quantification of α7 nAChR and gephyrin proteins in *Chat-IRES-Cre* and *Chat-Mecp2*$^{-/y}$ mice. **(C)** Immunostaining of the hippocampal pyramidal layer with PV interneurons and α7 nAChRs, showing the expression pattern of α7 nAChRs on PV GABAergic neurons and non-PV neurons. Error bars are means ± SEM. *P*-values were calculated by two-sided *t*-test. **P* < 0.05, ***P* < 0.01, ****P* < 0.001.

most prominent GABAergic neurons in the hippocampus, we co-stained α7 nAChRs and PV interneurons in the CA1 stratum pyramidal neurons. The results showed that α7 nAChRs were concentrated in PV GABAergic neurons, with little expression in non-PV neurons (Figure 4C).

The α7 nAChRs were highly expressed in the PV GABAergic neurons in the hippocampus (Figure 4C). To determine whether the expression of α7 nAChRs can regulate the excitability of PV GABAergic neurons [36], we performed whole-cell current-clamp recordings in acute hippocampal slices. Identification of PV GABAergic neurons by measuring their membrane properties and firing patterns was based on their distinctive characteristics. Neuronal excitability was measured by a series of 1-s step current injections. To exclude the possibility that the excitatory or inhibitory input to the PV neurons regulated its excitability, we blocked synaptic inputs with the N-methyl-D-aspartate receptor antagonist DL-2-amino-5-phosphonovaleric acid (DL-AP5; 50 μM), α-amino-3-hydroxy-5-methyl-4-isoxazole propionate (AMPA) and kainate receptor antagonist 6,7-dinitroquinoxaline-2,3-dione (DNQX; 20 μM), and $GABA_A$ receptor antagonist picrotoxin (100 μM). Under these conditions, bath application of 10 nM methyllycaconitine citrate (MLA), a potent and specific antagonist for α7 nAChRs, significantly increased the average interspike interval (ISI) of *Chat-IRES-Cre* mice, suggesting a direct effect of α7 nAChRs on the intrinsic properties of PV GABAergic neurons (Figure 5A). We then measured the excitability of PV GABAergic neurons in *Chat-Mecp2*$^{-/y}$ mice. Compared with the *Chat-IRES-Cre* mice, *Chat-Mecp2*$^{-/y}$ mice exhibited reduced intrinsic excitability of PV GABAergic neurons, as shown by prolonged ISI and decreased firing frequency (Figure 5B and Supplementary information, Figure S4A). We also measured passive membrane properties, including resting membrane potential, input resistance, membrane time constant and membrane capacitance, and found no significant differences between *Chat-Mecp2*$^{-/y}$ and *Chat-IRES-Cre* mice (Supplementary information, Figure S4B-S4E). To confirm that the expression of α7 nAChRs in PV GABAergic neurons was decreased

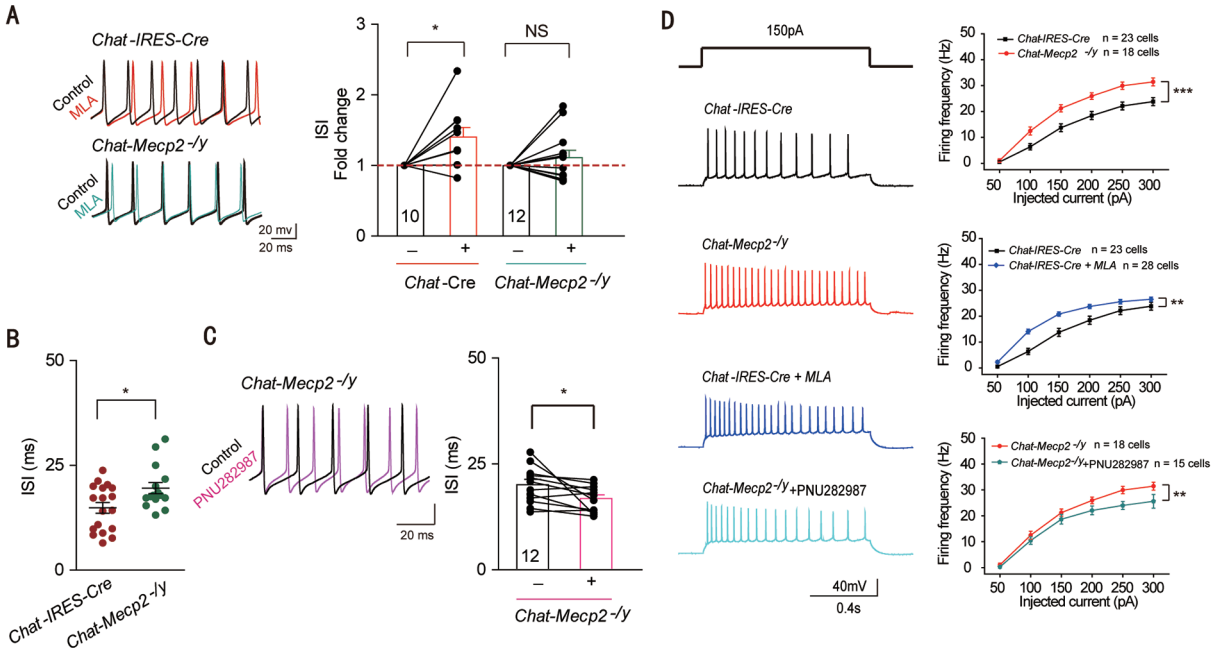

Figure 5 Downregulated GABAergic excitability and upregulated glutamatergic excitability mediated by α7 signaling in the hippocampal CA1 region of *Chat-Mecp2*$^{-/y}$ mice. **(A)** Left: Representative APs of PV GABAergic interneurons in hippocampal CA1 in *Chat-IRES-Cre* mice (top) and *Chat-Mecp2*$^{-/y}$ mice (bottom) before (black) and after (color) MLA (10 nM) treatment. Right: Normalized ISI of hippocampal PV GABAergic interneurons before and after bath application of 10 nM MLA in both *Chat-IRES-Cre* and *Chat-Mecp2*$^{-/y}$ mice. *P*-values were calculated by paired *t*-test for each genotype. **(B)** Summary histogram of ISI of PV GABAergic interneurons in slices from *Chat-IRES-Cre* and *Chat-Mecp2*$^{-/y}$ mice (two-sided *t*-test). **(C)** Left: Representative APs of PV GABAergic interneurons in hippocampal CA1 in *Chat-Mecp2*$^{-/y}$ mice before (black) and after (color) PNU282987 (1 μM) treatment. Right: Plot of ISI before and after application of PNU282987 (1 μM). *P*-values were calculated by paired *t*-test. **(D)** Voltage responses to various current injection steps (1 s) in pyramidal neurons from *Chat-IRES-Cre* and *Chat-Mecp2*$^{-/y}$ mice at baseline or in the presence of MLA or PNU282987. Representative traces (left) and summary graph (right) show the firing frequency of pyramidal neurons from *Chat-IRES-Cre* and *Chat-Mecp2*$^{-/y}$ mice (two-way repeated measures ANOVA). Error bars are means ± SEM. **P* < 0.05, ****P* < 0.001.

in *Chat-Mecp2*$^{-/y}$ mice, we assessed the effect of MLA, a specific α7 nAChR blocker, on hippocampal slices from *Chat-Mecp2*$^{-/y}$ mice. In contrast to the increase in ISI by MLA treatment in the control mice, there was no significant change in ISI following MLA application in *Chat-Mecp2*$^{-/y}$ mice (Figure 5A). In addition, bath application of PNU282987, a selective α7 nAChR agonist, to stimulate the remaining α7 nAChRs in *Chat-Mecp2*$^{-/y}$ mice decreased the ISI of PV GABAergic neurons (Figure 5C). These results indicate that α7 nAChRs were critical for the excitability of PV neurons, and the expression of α7 nAChRs on PV neurons was downregulated in *Chat-Mecp2*$^{-/y}$ mice. To test whether α7 nAChRs can regulate the excitability of pyramidal neurons through PV interneurons in the hippocampus, we compared the excitability of CA1 pyramidal neurons from the control and *Chat-Mecp2*$^{-/y}$ mice by examining the frequency of action potentials (APs). Pyramidal neurons were recorded under physiological status. The frequency of APs was significantly increased in *Chat-Mecp2*$^{-/y}$ mice after current injections of various amplitudes compared with that in *Chat-IRES-Cre* mice (Figure 5D). Bath application of MLA in the hippocampal slices of *Chat-IRES-Cre* mice increased the excitability of pyramidal neurons. Treatment with PNU282987 in *Chat-Mecp2*$^{-/y}$ mice decreased the excitability of pyramidal neurons (Figure 5D).

Taken together, these data suggest that conditional deletion of *Mecp2* in cholinergic neurons might change the expression level of ChAT. Altered ACh content in the hippocampus could influence the expression level of α7 nAChRs in PV GABAergic neurons. Due to the decreased expression of α7 nAChRs, PV neurons exhibited reduced excitability, as shown by prolonged ISI. Since pyramidal neurons can be innervated by PV GABAergic interneurons, the excitability of CA1 pyramidal neurons was significantly increased after current injections of

various amplitudes.

Increased seizure susceptibility in Chat-Mecp2$^{-/y}$ mice was rescued by activation of α7 nAChRs

A shift in the balance between excitation and inhibition can lead to neuronal hyperexcitation or even epilepsy. Thus, we determined whether increased excitability in pyramidal neurons caused hyperexcitable network activity. Electroencephalographic (EEG) recordings in freely moving mice revealed that *Chat-Mecp2$^{-/y}$* mice suffered frequent hyperexcitability discharges (Figure 6A and 6B). Clinical studies have shown that nearly 80% of RTT patients suffer recurrent seizures [6]. We also measured seizure susceptibility by administering the common convulsant agent pilocarpine, a non-selective mAChR agonist, to *Chat-IRES-Cre* and *Chat-Mecp2$^{-/y}$* mice (Figure 6A). We quantified the percentage of mice that developed status epilepticus, which was nearly half within each genotype (Figure 6C). However, *Chat-Mecp2$^{-/y}$* mice had a shorter onset time than *Chat-IRES-Cre* mice (Figure 6D). Application of PNU282987 in the CA1 of the hippocampus in *Chat-Mecp2$^{-/y}$* mice 15 min before the injection of pilocarpine prolonged the onset time for seizures, indicating the involvement of α7 nAChRs in seizure susceptibility manifested in *Chat-Mecp2$^{-/y}$* mice (Figure 6).

α7 nAChRs in the hippocampus could be molecular mediators of the phenotypes in Chat-Mecp2$^{-/y}$ mice

Reduced α7 nAChR function and signaling may contribute to part of RTT-like phenotypes in *Chat-Mecp2$^{-/y}$* mice. To test this hypothesis, we used PNU282987 to selectively activate α7 nAChRs in the CA1 of the hippocampus (Figure 7A). PNU282987 rescued altered anxiety- and depression-related behavior in *Chat-Mecp2$^{-/y}$* mice (Figure 7B-7E). In addition, PNU282987-treated *Chat-Mecp2$^{-/y}$* mice showed improved social interaction in the three-chamber test (Figure 7F). Nicotine appears to be the primary agent in cigarettes that can target all nAChRs, including α7 nAChRs. Application of nicotine also rescued the behav-

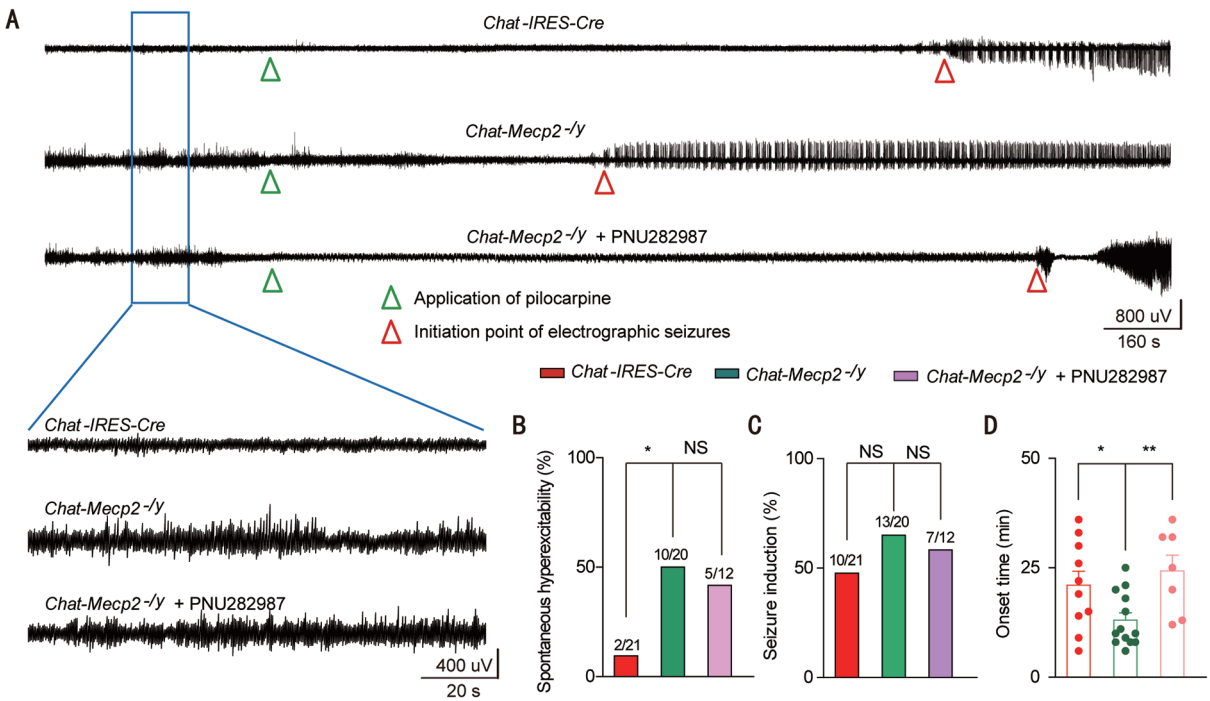

Figure 6 Application of PNU282987 in the CA1 of the hippocampus suppressed seizure susceptibility in *Chat-Mecp2$^{-/y}$* mice. **(A)** Representative EEG traces recorded from freely moving *Chat-IRES-Cre* and *Chat-Mecp2$^{-/y}$* mice or PNU282987-treated *Chat-Mecp2$^{-/y}$* mice. Bottom: Enlarged EEG traces showing baseline excitability discharges. **(B)** Incidence of spontaneous hyperexcitability in *Chat-Mecp2$^{-/y}$* mice and their control littermates (*Chat-IRES-Cre*) or PNU282987-treated *Chat-Mecp2$^{-/y}$* mice. χ^2 test was used. **(C)** Percentage of pilocarpine-induced seizures in *Chat-IRES-Cre* and *Chat-Mecp2$^{-/y}$* mice or PNU282987-treated *Chat-Mecp2$^{-/y}$* mice. χ^2 test was used. **(D)** Quantitative analysis of onset time for seizure induction in *Chat-IRES-Cre* and *Chat-Mecp2$^{-/y}$* mice or PNU282987-treated *Chat-Mecp2$^{-/y}$* mice. Two-way ANOVA was used. Error bars are means ± SEM. **P* < 0.05, ***P* < 0.01, ****P* < 0.001.

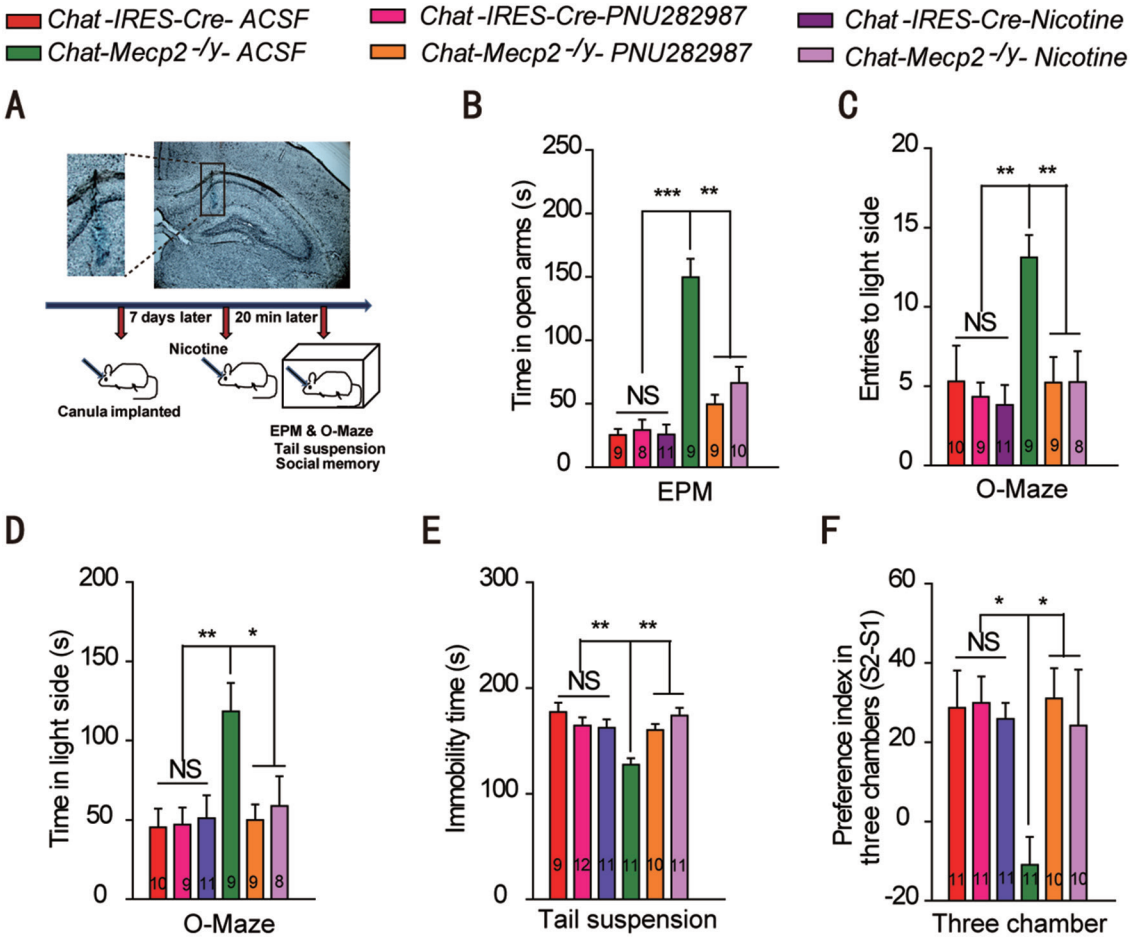

Figure 7 Delivery of nicotine or PNU282987 in the hippocampus rescued behavioral deficits manifested in *Chat-Mecp2*$^{-/y}$ mice. **(A)** Top: Microinjection of toluidine blue into the CA1 of the hippocampus. Shown is a representative section after injection. Bottom: Schematic of the protocol. **(B-D)** Anxiety-related behavior examined by the elevated plus-maze (EPM) and zero-maze. Data are time spent in the open arms of the EPM as well as number of entries and time spent in the lit compartment of the zero-maze. **(E)** Depression-related behavior was measured by the immobility time displayed in tail suspension. **(F)** Social behavior was measured as the ratio of interaction time with a stranger mouse to interaction time with a familiar mouse in the three-chamber test. *P*-values were calculated by two-way ANOVA (genotype × trial) with Bonferroni's *post hoc* comparison. Error bars are means ± SEM. **P* < 0.05, ***P* < 0.01, ****P* < 0.001.

ioral phenotypes of *Chat-Mecp2*$^{-/y}$ mice (Figure 7B-7F). Long-term delivery of nicotine in the hippocampus also improved social memory in WT mice (Supplementary information, Figure S5). These results suggest that the α7 nAChRs in the hippocampus might be potential molecular mediators for RTT phenotypes.

Discussion

In this study, we presented evidence that loss of MeCP2 in cholinergic neurons caused part of RTT-like phenotypes via α7 nAChRs in the hippocampus. First, conditional deletion of *Mecp2* from cholinergic neurons resulted in several RTT-like phenotypes such as impaired social interaction, altered anxiety-related behavior and epilepsy susceptibility, suggesting the involvement of the cholinergic systems in the pathogenesis of RTT. Second, reactivation of *Mecp2* in BF cholinergic neurons, rather than CPu cholinergic neurons, improved phenotypic severity in *Chat-Mecp2*$^{-/y}$ mice, implicating the crucial role of the BF cholinergic system in these phenotypes. Third, both the activity of cholinergic neurons and the expression of ChAT were decreased in the BF and α7 nAChR signaling was strongly impaired in the hippocampus of *Chat-Mecp2*$^{-/y}$ mice. Of particular importance, intracerebral infusion of PNU282987 or nicotine rescued the

behavioral defects in *Chat-Mecp2*$^{-/y}$ mice. These findings suggest that MeCP2 is critical for normal function of cholinergic neurons and dysfunction of cholinergic neurons can contribute to numerous neuropsychiatric phenotypes.

Earlier studies showed that loss of *Mecp2* from serotoninergic neurons causes increased aggression, whereas loss from dopaminergic neurons leads to motor incoordination [16]. Furthermore, loss from forebrain excitatory neurons can lead to cortical hyperexcitation and seizures [20], and selective deletion in GABAergic neurons can reproduce most RTT phenotypes, including autism-like stereotypes [17]. These studies suggest that different neuronal types in various brain regions are involved in the pathogenesis of RTT. What is the specific role that cholinergic systems play in RTT or to what extent do cholinergic neurons contribute to this devastating disorder? Previous studies showed that cholinergic hypofunction in *Mecp2-308* mice, a mouse line that expresses the truncated form of the *Mecp2* gene, was associated with milder phenotypes, which could be improved by postnatal choline supplementation [37]. However, the use of *Mecp2*-null mice may mask the direct effect of MeCP2 dysfunction in specific circuits. Moreover, accumulating evidence suggests that dysfunction of the cholinergic system may underlie autism-related behavioral symptoms and the etiology of anxiety-related behaviors [26, 32]. In the present study, we showed that conditional deletion of *Mecp2* from cholinergic neurons resulted in certain RTT-related phenotypes, including impaired social interaction and seizure penetrance. Surprisingly, despite the role that the cholinergic system plays in motor control, we did not observe any deficit in motor activity, a phenotype typically seen in RTT models. Moreover, conditional deletion of *Mecp2* from cholinergic neurons did not affect the hippocampus-dependent learning and memory in the Morris water maze, despite the defect of cholinergic signaling in the hippocampus of *Chat-Mecp2*$^{-/y}$ mice. In addition, the aberrant behavior of *Chat-Mecp2*$^{-/y}$ mice in the tail suspension and forced swim tests is not typical in RTT patients, suggesting the possible involvement of MeCP2 in other neurological diseases besides RTT, such as mood disorder. These results indicate for the first time the direct involvement of the cholinergic system in some aspects of RTT pathogenesis. However, whether the cholinergic system is involved in breathing function and other RTT-like phenotypes remains to be explored.

Cholinergic neurons in the brain include projection neurons that innervate distal areas and interneurons that are interspersed among their cellular targets. The BF cholinergic neurons project diffusely to the entire cortex and hippocampus, mediating attention, arousal and even mood [38, 39]. Cholinergic interneurons in the striatum appear to act in motor regulation, associative plasticity and reward-dependent learning [40, 41]. Here, we indicated that deletion of *Mecp2* from cholinergic neurons throughout the adult mouse brain resulted in specific behavioral deficits. Delayed reactivation of *Mecp2* in the BF cholinergic neurons improved the phenotype severity manifested in the *Chat-Mecp2*$^{-/y}$ mice. However, reactivation of *Mecp2* in the CPu cholinergic interneurons did not cause similar phenotypes, highlighting the regional specificity of behavioral phenotypes and the important role of MeCP2 in BF cholinergic neurons. It is interesting to note that only 30% re-expression in BF cholinergic neurons rescued almost all behavior deficits in *Chat-Mecp2*$^{-/y}$ mice (Supplementary information, Figure S2 and Figure 2), suggesting that MeCP2 in BF cholinergic neurons is essential, with only 30% required for normal function and behavior. There are three major neuronal types in the BF: cholinergic, glutamatergic and GABAergic. These cholinergic neurons are known to project widely and diffusely, innervating neurons throughout the CNS. They also exhibit extensive local collaterals terminating on GABAergic neurons within the BF, thus controlling sleep and wakefulness [42, 43]. We identified the fundamental role of the septo-hippocampal cholinergic system in the development of the behavioral deficits in *Chat-Mecp2*$^{-/y}$ mice. However, whether cholinergic circuitries, besides septo-hippocampal projection, are involved in the phenotypes of *Chat-Mecp2*$^{-/y}$ mice still require investigation.

The hippocampus receives dense cholinergic projections mainly from the BF [44]. Cholinergic signaling in the hippocampus plays a crucial role in memory processing and mood regulation [37]. The hippocampus expresses a wide variety of nAChRs, with the α7 subunits being mainly expressed [45]. Immunofluorescence studies on cultured hippocampal neurons show that rather than glutamatergic principal cells, α7 nAChRs are densely expressed in GABAergic interneurons in the hippocampus [35]. PV interneurons have a fast-spiking pattern and are the dominant inhibitory system in the hippocampus. In the present study, we showed evidence that α7 nAChRs were clustered on hippocampal PV interneurons and were decreased in *Chat-Mecp2*$^{-/y}$ mice. Nicotinic receptors function as non-selective, excitatory cation channels regulating the excitability of neural circuits [36]. We showed that the application of MLA to block α7 nAChRs on PV neurons directly decreased the excitability of these neurons. Consistent with our previous biochemical findings, *Chat-Mecp2*$^{-/y}$ mice had reduced intrinsic excitability of PV interneurons, as shown by prolonged ISI, indicating decreased α7 nAChR expression in the PV neu-

rons. PV interneurons preferentially project axons onto the peri-somatic region of target neurons, regulating the output of pyramidal neurons [46]. The excitability of CA1 pyramidal neurons was significantly increased after current injections of various amplitudes in *Chat-Mecp2*$^{-/y}$ mice (Figure 8). EEG recordings also revealed that *Chat-Mecp2*$^{-/y}$ mice suffered frequent hyperexcitability discharges. In addition, our results showed that *Chat-Mecp2*$^{-/y}$ mice were more prone to pilocarpine-induced epilepsy, a predominant feature of RTT patients [31]. Application of PNU282987 or nicotine rescued the seizure susceptibility of *Chat-Mecp2*$^{-/y}$ mice, suggesting impairment of nicotinic signaling in the hippocampus of *Chat-Mecp2*$^{-/y}$ mice. However, since the BF cholinergic neurons project diffusely to other regions, such as the cortex, rather than the hippocampus, we cannot exclude the possibility that other brain regions may also be involved in these phenotypes. In addition, as many other cholinergic receptors are also expressed in the hippocampal region, we cannot rule out the possible effect of non-α7 AChRs on the phenotypes manifested in *Chat-Mecp2*$^{-/y}$ mice.

Previous studies revealed that MeCP2 deficiency in GABAergic neurons leads to reduced GABAergic signaling, which results in specific RTT phenotypes such as hyperexcitatory EEG recordings [17]. MeCP2 regulates a number of genes, including *CHRNA7*, which encode cholinergic α7 nAChRs [47, 48]. This raises the possibility that the observed phenotype in *Viaat-Mecp2*$^{-/y}$ mice (deletion of *Mecp2* from GABAergic neurons) might be due to deficient α7 nAChR signaling in GABAergic neurons, in addition to impaired GABA synthesis. However, more work is required to test this hypothesis. Nicotine is an nAChR agonist, and its application in the hippocampus rescued social deficits seen in the *Mecp2* conditional knockout mice. Our results suggest that α7 nAChRs might be a potential target for the treatment of RTT. However, we cannot exclude other potential factors that might be involved in the pathogenesis of *Chat-Mecp2*$^{-/y}$ mice. For example, chronic administration of nicotine may upregulate nAChRs through enhanced intracellular maturation [19]. Future work is required before these findings can be applied biomedically. Other mechanisms besides α7 signaling may also be involved in the development of these phenotypes.

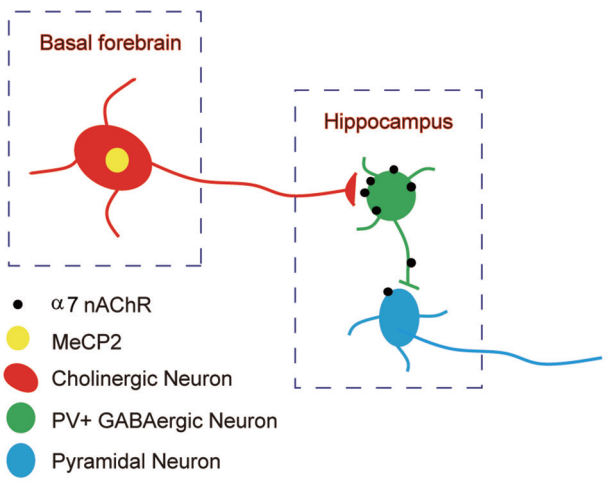

Figure 8 Schematic diagram of the working model.

Materials and Methods

Mice and reagents

To specifically delete *Mecp2* in ChAT-positive cholinergic neurons, *Chat-Mecp2*$^{-/y}$ mice were generated by breeding female *Mecp2*$^{flox/-}$ mice (Jax No. 006847) with *Chat-IRES-Cre* (Jax No. 006410) heterozygous male mice. To assist electrophysiological recordings of cholinergic neurons, *Chat-IRES-Cre* and *Chat-Mecp2*$^{-/y}$ mice were crossed with Ai9 mice (Jax No. 7909) to specifically label cholinergic neurons with tdTomato. Only male offspring were used in the experiments. All mice belonged to the C57BL/6J strain and were housed under a 12 h light/dark cycle with *ad libitum* access to food and water. Mouse care and use followed the guidelines of the Animal Advisory Committee at Zhejiang University and the US National Institutes of Health Guidelines for the Care and Use of Laboratory Animals.

Primary antibodies used were rabbit monoclonal anti-MeCP2 (Cell Signaling Technology, USA, Cat#: 3456s), rabbit polyclonal anti-α7 nAChR (Santa Cruz Biotechnology, USA, Cat#: sc-5544), goat polyclonal anti-ChAT (Millipore, USA, Cat#: AB144P), mouse monoclonal anti-parvalbumin (PV235, Swant, Switzerland), rabbit polyclonal anti-GAPDH (Cell Signaling Technology, Cat#: 5014S), mouse monoclonal anti-GAD65 (Santa Cruz Biotechnology, Cat#: sc-32270) and goat polyclonal anti-gephyrin (Santa Cruz Biotechnology, Cat#: sc-6411). DAPI was used to stain nuclei.

DL-AP5, DNQX and picrotoxin were purchased from Tocris Bioscience (USA), MLA was purchased from Abcam (UK), and pilocarpine, nicotine and PNU282987 were purchased from Sigma-Aldrich (USA). Chemicals were dissolved in dimethyl-sulfoxide (DMSO, Sigma, USA) when necessary. When applied to brain slices, the final concentration of DMSO was < 0.01%.

Behavior assays

Mice at 9-15 weeks of age were used for all tests. We first evaluated the mice for general health, including body weight and fur appearance. The mice were then transferred to the animal facility 1 week before the behavioral tests. They were allowed to habituate to the testing room for 30 min before test commencement. All behavioral tests were carried out blind to genotype with age-matched male littermates.

Motor, anxiety- and depression-related behavioral tests

Open field: spontaneous locomotor activity was assessed over 15 min in an arena (45 cm × 45 cm × 45 cm). Locomotor activity was evaluated as total distance traveled. Anxiety-like behavior was

defined by the distance traveled in the center compared with the distance traveled in the perimeter of the arena.

EPM: The EPM apparatus was comprised of two open arms (30 cm × 5 cm) and two closed arms (30 cm × 5 cm × 20 cm) elevated 50 cm above the floor. Mice were placed in the center facing one of the two open arms and allowed to explore for 6 min. Anxiety-like behavior was assessed by time and distance traveled in the open arms.

LD box: The LD box consisted of a clear Plexiglas chamber (30 cm × 15 cm × 5 cm) separated from a covered black chamber (30 cm × 15 cm × 5 cm) by a black partition with a small opening. The lighting was maintained at 700 lux. Mice were placed in the dark box and allowed to explore the apparatus for 5 min. The time spent in the lit box was measured.

Zero-maze: The zero-maze was elevated 50 cm above the floor and was indirectly illuminated at 100 lux. Mice were introduced to a closed area of the maze and video-taped for 5 min. Anxiety-like behavior was assessed by the number of visits and duration in the open arms.

Tail suspension: Mice were gently suspended by the tail and video-taped for 6 min. Immobility was defined as no movement except for respiration and was counted as an index for depression.

Forced swim: Mice were placed in clear glass beakers filled with water at around 25 °C. A pretest session of 15 min was included to accentuate the different behavior in the 5 min test. Immobility was defined as minimal movement made by the mouse to stay afloat. Mice were returned to their home cage at the end of the test.

Social interaction tests

Open field social interaction test: A paired novel mouse was introduced to the home cage of the test mouse for 10 min. Behaviors were view-recorded and analyzed to assess active interaction time of the test mouse with a novel mouse. During the test, the investigators remained outside the testing room.

Three-chamber test: The three-chamber social test was conducted as described elsewhere [7] with minor modifications. The apparatus consisted of a rectangular Plexiglas box (60 cm × 35 cm × 10 cm) evenly divided into three chambers with partitions. Time spent in each chamber and time spent in close interaction with a stranger mouse were recorded for analysis. "Close interaction" was defined as a 5 cm radius proximal to each wire cage where test mice initiated active interaction with a stranger mouse. Target subjects (stranger 1 and stranger 2) were 9-10-week old males habituated to being placed inside the cages for a week before the test. (A) Habituation: the test mouse was placed in the middle chamber and allowed to explore for 5 min. Each side contained an empty wire cage with a weighted bottle on top of each cage to prevent climbing by the test mice. The total time that the test mouse spent in each side was measured. (B) Sociability: an age- and gender-matched stranger 1 was introduced to the wire cage located on one side. The empty cage served as an inanimate object with no social valence. The test mouse was placed in the center chamber and allowed to explore the entire apparatus for 5 min. Total time spent in the chamber and in close interaction with the cages was recorded and the preference index (S1-E) was measured as the ratio of (S1-E) to (S1+E). (C) Social memory: a new stranger 2 was introduced to the other empty cage. The test mouse spent another 5 min in exploring the entire apparatus. Total time spent in the chamber and in close interaction with the cages was recorded and the preference index (S2-S1) was measured as the ratio of (S2-S1) to (S2+S1).

Nest building test: A single-housed test was conducted in which each singularly-housed mouse was given the same amount of roll paper on the first day. The shape of the nests built by the test mice was pictured and evaluated 48 h later.

Morris water maze: The Morris water maze is widely used to study spatial learning and memory. This test was conducted as previously published [17], with a few modifications. Each mouse was given three trials a day for 4 consecutive days. The time taken to locate the platform was measured. After all animals completed 12 trials, they were given a probe trial in which the platform was removed from the pool. Each animal was allowed 30 s to search the pool. The amount of time that each animal spent in the target quadrant was recorded and analyzed.

Immunohistochemistry

Mice were anesthetized and transcardially perfused with 4% paraformaldehyde in phosphate-buffered saline (PBS). Whole brains were removed and fixed with paraformaldehyde at 4 °C overnight. The fixed brains were then cryoprotected in 30% sucrose in PBS. We cut 35-μm-thick sections from regions of interest on a freezing microtome according to anatomical landmarks. For immunolabeling, brain sections were treated with 10% (vol/vol) normal donkey serum in PBS containing 0.3% Triton X-100. The brain sections were then incubated with antibodies of anti-Mecp2 (1:200), anti-ChAT (1:100), anti-α7 nAChR (1:100), and anti-parvalbumin (1:1 000) at 4 °C overnight. Immunoreactivity was imaged with the secondary antibodies of Alexa Fluor 594 donkey anti-mouse, Alexa Fluor 633 donkey anti-goat and Alexa Fluor 488 donkey anti-rabbit lgG (1:400). Immunofluorescent images were visualized by confocal microscopy (FV1000 Laser Scanning Confocal Microscope, USA).

Western blot analysis

We homogenized BF and hippocampal tissue in lysis buffer (Beyotime Biotechnology, China) containing 1 mM protease inhibitor PMSF (Beyotime Biotechnology). Supernatants were collected after centrifugation for 10 min at 15 000 rpm. After determining the protein concentration with Bradford's solution (Beyotime Biotechnology), samples containing equivalent amounts of protein were boiled for 5 min in loading buffer (Beyotime Biotechnology). SDS-PAGE was carried out and the proteins were transferred to an Immobilon PVDF membrane (Millipore) for 100 min at 300 mA. After blocking with TBST solution (50 mM Tris-HCl, pH 7.5, 150 mM NaCl, and 0.1% Tween 20) containing 5% skimmed milk for 1 h at room temperature, membranes were incubated with primary antibodies of anti-α7 nAChR (1:100), anti-GAPDH (1:5 000), anti-ChAT (1:1 000), anti-GAD65 (1:500), and anti-gephyrin (1:500) at 4 °C overnight. After washing with TBST, blots were incubated with secondary antibodies (1:7 500) for 1 h at room temperature. We quantified band intensities using the US National Institutes of Health Images program and normalized all bands to control values.

In vitro electrophysiology

Acute slice preparation: Coronal slices (350 μm) of the hippocampus from 17-22-postnatal day mice were prepared with a Vibroslice (Leica VT 1000S, USA) in ice-cold artificial cerebro-

spinal fluid (ACSF; composition in mM: 125 NaCl, 3 KCl, 1.25 NaH_2PO_4, 2 $MgSO_4$, 2 $CaCl_2$, 25 $NaHCO_3$, 10 glucose). The slices were allowed to recover in ACSF at 33 °C for 30 min and then kept at room temperature until recording. All solutions were saturated with 95% O_2 and 5% CO_2.

Electrophysiological recordings: Neurons were visualized with an infrared-sensitive CCD camera and 40× water-immersion lens (ECLIPSE FN1, Nikon, Japan) and recorded using whole-cell techniques (MultiClamp 700B Amplifier, Digidata 1440A analog-to-digital converter, USA) and pClamp 10.2 software (Axon Instruments/Molecular Devices, USA). For AP recordings, neurons were patched with electrodes containing the following (in mM): 130 potassium gluconate, 20 KCl, 10 HEPES buffer, 4 Mg-ATP, 0.3 Na-GTP, 10 disodium phosphocreatine and 0.2 EGTA, pH 7.25 with KOH, 288 mOsm. When filled with intracellular solution, patch electrode resistance ranged from 3 to 5 MΩ. ISI, defined as the average intervals between sequential APs in a train elicited by a 1 s suprathreshold current of 400 pA, was used to quantify the excitability of PV GABAergic neurons. A series of 1 s suprathreshold currents of 50-300 pA were used to quantify the excitability of pyramidal neurons. The holding for AP recording was −70 mV. Membrane time constant (Tau) was measured with a single exponential fit of the voltage deflection produced by a small hyperpolarizing current injection from the resting membrane potential. The spontaneous firing of cholinergic neurons was recorded at resting membrane potential. If neurons were not spontaneously active, we discarded the recording. Recordings were Bessel-filtered at 10 KHz and sampled at 100 KHz. Access resistance was continuously monitored for each cell. Only neurons with series resistance below 20 MΩ and changing < 20% throughout the recording were used for analysis. All analyses were performed in Clampfit version 10.5 (Axon Instruments, USA).

Virus preparation and delivery

To re-express *Mecp2* in cholinergic neurons, we injected the AAV8/Mecp2 vector into the BF (800 nl) or CPu (1 μl each side) of *Chat-Mecp2*$^{-/y}$ mice and the AAV8/GFP vector into *Chat-IRES-Cre* and *Chat-Mecp2*$^{-/y}$ mice. The plasmids were gifts from Dr Zilong Qiu (Institute of Neuroscience, Shanghai). 6-8-week-old male mice were anesthetized with 2% isoflurane and mounted on a custom-built mouse stereotaxic device during surgery. Heart rate and body temperature were continuously monitored. Eye drops were applied to prevent drying. The animals received stereotaxic injections of AAV into the CPu and BF. Coordinates used for BF injection were AP + 0.98 mm and DV − 4.5 mm and for CPu injection were AP + 0.98 mm, ML ± 1.25 mm and DV − 3.1 mm. The AAV vector was delivered with a glass microelectrode into the target coordinates over a 10 min period. Three weeks after the introduction of the viral vector, the behavioral tests were performed.

EEG and electromyogram recordings

Male ChAT-ChR2 mice (8-12-week old) were anesthetized with 2% isoflurane and placed in a stereotaxic frame. We implanted four stainless-steel screws in the mouse skulls, including two in the temporal lobe for EEG contact, one in the cerebellar for grounding and one for mechanical support. For EMG recordings, two polyester enameled wire electrodes were inserted into the neck musculature. After 7 days of post-surgical recovery, EEG and EMG activities were recorded in freely moving mice. EEGs of freely moving mice were continuously recorded for 30 min before drug administration to establish baselines, and were recorded for another 30 min after pilocarpine induction to determine the effect of the drug on the occurrence of epilepsy in each genotype. Generalized seizures were defined by repetitive epileptiform spiking activity (≥ 3 Hz) and persistence for at least 3 s. Data were collected and analyzed using TM_WAVE software version 2.0 (Chengdu Technology, China).

Drug and treatment procedures

To rescue the RTT phenotypes with the application of nicotine or PNU282987, a cannula with a diameter of only 0.34 mm was implanted into the CA1 of the hippocampus. For each mouse, the cannula was secured using dental cement. After a week of recovery, the mice were subjected to different behavioral tests. Twenty minutes before each experiment, 0.2 μl of 1 nM nicotine or 1 M PNU282987 was delivered. For seizure induction, pilocarpine was injected intraperitoneally at a dosage of 200 mg/kg. PNU282987 was delivered 15 min before the injection of pilocarpine.

Statistical analyses

All data were analyzed using commercially available statistical software packages (Prism 5 and SPSS, version 17.0). Student's *t*-test was used for data sets including two independent groups. For example: Figure 1B, 1H-1J; Figure 3; Figure 4B; Figure 5B; Supplementary information, Figure S1F-S1H and S1L-S1N; Supplementary information, Figure S3; Supplementary information, Figure S4B-S4I and Supplementary information, Figure S5. For data sets including three or more groups with one factor, one-way analysis of variance (ANOVA) was applied to analyze the differences. For example: Figure 1D-1I; Figure 7 and Supplementary information, Figure S1B-S1E, S1I-S1K, S1P. Two-way ANOVA (genotype × trial) was used to analyze groups with two factors. For example: Figure 2; Figure 6D and Figure 7. For comparison of pre- and post-medicine application (Figure 5A and 5C), paired-sample *t*-tests were used to calculate the effect of MLA and PNU282987 application on each genotype. For the change in firing frequency elicited by current injections (Figure 5D and Supplementary information, Figure S4A), statistical significance was determined by two-way repeated-measures ANOVA. For comparing different percentages between samples (Figure 6B and 6C), Pearson's χ^2 test was applied. Data were means ± SEM (n = number of individual samples).

Acknowledgments

We are grateful to ZL Qiu (Institute of Neuroscience, Chinese Academy of Sciences) for providing the AAV8/Mecp2 plasmid. We thank AM Bao (Zhejiang University) for technical assistance, and K-XL and JZ for suggestions on this project. This work was supported by the National Natural Science Foundation of China for Distinguished Young Scientists (81225007), Key Project of the National Natural Science Foundation of China (31430034), Major Research Plan of the National Natural Science Foundation of China (91432306), Funds for Creative Research Groups of China (81221003), Program for Changjiang Scholars and Innovative Research Team in University, and Fundamental Research Funds for the Central Universities. This work was also sponsored by the Zhejiang Province Program for Cultivation of High-level Health

Talents.

Author Contributions

YZ conducted the experiments, analyzed data and wrote the manuscript; S-X C conducted the experiments and collected the data. PS performed the studies on the mouse model; H-Y H and C-H Y performed part of the behavioral tests; X-J C and C-J S conducted part of the gene identification; X-D W, ZC, DKB and SD contributed experimental suggestions. X-M L supervised all phases of the project.

Competing Financial Interests

The authors declare no competing financial interests.

References

1 Chahrour M, Zoghbi HY. The story of Rett syndrome: from clinic to neurobiology. *Neuron* 2007; **56**:422-437.
2 Lyst MJ, Bird A. Rett syndrome: a complex disorder with simple roots. *Nat Rev Genet* 2015; **16**:261-275.
3 Hagberg B. Retts syndrome: prevalence and impact on progressive severe mental-retardation in girls. *Acta Paediatr Scand* 1985; **74**:405-408.
4 Mount RH, Hastings RP, Reilly S, Cass H, Charman T. Behavioural and emotional features in Rett syndrome. *Disabil Rehabil* 2001; **23**:129-138.
5 Naidu S, Johnston MV. Neurodevelopmental disorders: clinical criteria for Rett syndrome. *Nat Rev Neurol* 2011; **7**:312-314.
6 Jian L, Nagarajan L, de Klerk N, *et al.* Predictors of seizure onset in Rett syndrome. *J. Pediatr.* 2006; **149**:542-547.
7 Neul JL, Kaufmann WE, Glaze DG, *et al.* Rett Syndrome: revised diagnostic criteria and nomenclature. *Ann Neurol* 2010; **68**:944-950.
8 Amir RE, Van den Veyver IB, Wan M, *et al.* Rett syndrome is caused by mutations in X-linked MECP2, encoding methyl-CpG-binding protein 2. *Nat Genet* 1999; **23**:185-188.
9 Moretti P, Zoghbi HY. MeCP2 dysfunction in Rett syndrome and related disorders. *Curr Opini Genet Dev.* 2006; **16**:276-281.
10 Chen RZ, Akbarian S, Tudor M, Jaenisch R. Deficiency of methyl-CpG binding protein-2 in CNS neurons results in a Rett-like phenotype in mice. *Nat Genet* 2001; **27**:327-331.
11 Guy J, Hendrich B, Holmes M, Martin JE, Bird A. A mouse Mecp2-null mutation causes neurological symptoms that mimic Rett syndrome. *Nat Genet* 2001; **27**:322-326.
12 Shahbazian M, Young J, Yuva-Paylor L, *et al.* Mice with truncated MeCP2 recapitulate many Rett syndrome features and display hyperacetylation of histone H3. *Neuron*, 2002; **35**:243-254.
13 Samaco RC, Mandel-Brehm C, McGraw CM, *et al.* Crh and Oprm1 mediate anxiety-related behavior and social approach in a mouse model of MECP2 duplication syndrome. *Nat Genet* 2012; **44**:206-211.
14 Zoghbi HY. Postnatal neurodevelopmental disorders: meeting at the synapse? *Science* 2003; **302**:826-830.
15 Fyffe SL, Neul JL, Samaco RC, *et al.* Deletion of *Mecp2* in Sim1-expressing neurons reveals a critical role for MeCP2 in feeding behavior, aggression, and the response to stress. *Neuron* 2008; **59**:947-58
16 Samaco RC, Mandel-Brehm C, Chao HT, *et al.* Loss of MeCP2 in aminergic neurons causes cell-autonomous defects in neurotransmitter synthesis and specific behavioral abnormalities. *Proc Natl Acad Sci USA* 2009; **106**:21966-21971.
17 Chao HT, Chen H, Samaco RC, *et al.* Dysfunction in GABA signalling mediates autism-like stereotypes and Rett syndrome phenotypes. *Nature* 2010; **468**:263-269.
18 Deng JV, Rodriguiz RM, Hutchinson AN, *et al.* MeCP2 in the nucleus accumbens contributes to neural and behavioral responses to psychostimulants. *Nat Neurosci* 2010; **13**:1128-1136.
19 He LJ, Liu N, Cheng XJ, *et al.* Conditional deletion of Mecp2 in parvalbumin-expressing GABAergic cells results in the absence of critical period plasticity. *Nat Commun* 2014; **5**:5036.
20 Zhang W, Peterson M, Beyer B, Frankel WN, Zhang ZW. Loss of MeCP2 from forebrain excitatory neurons leads to cortical hyperexcitation and seizures. *J Neurosci* 2014; **34**:2754-2763.
21 Garg SK, Lioy DT, Cheval H, *et al.* Systemic delivery of MeCP2 rescues behavioral and cellular deficits in female mouse models of Rett syndrome. *J Neurosci* 2013; **33**:13612-13620.
22 Lang M, Wither RG, Brotchie JM, *et al.* Selective preservation of MeCP2 in catecholaminergic cells is sufficient to improve the behavioral phenotype of male and female Mecp2-deficient mice. *Hum Mol Genet* 2013; **22**:358-371.
23 Lang M, Wither RG, Colic S, *et al.* Rescue of behavioral and EEG deficits in male and female Mecp2-deficient mice by delayed Mecp2 gene reactivation. *Hum Mol Genet* 2014; **23**:303-318.
24 Mellios N, Woodson J, Garcia RI, *et al.* beta2-Adrenergic receptor agonist ameliorates phenotypes and corrects microRNA-mediated IGF1 deficits in a mouse model of Rett syndrome. *Proc Natl Acad Sci USA* 2014; **111**:9947-9952.
25 Mineur YS, Obayemi A, Wigestrand MB, *et al.* Cholinergic signaling in the hippocampus regulates social stress resilience and anxiety- and depression-like behavior. *Proc Natl Acad Sci USA* 2013; **110**:3573-3578.
26 Sarter M, Parikh V. Choline transporters, cholinergic transmission and cognition. *Nat Rev Neurosci* 2005; **6**:48-56.
27 Steinlein OK, Mulley JC, Propping P, *et al.* A missense mutation in the neuronal nicotinic acetylcholine-receptor alpha-4 subunit is associated with autosomal-dominant nocturnal frontal-lobe epilepsy. *Nat Genet* 1995; **11**:201-203.
28 Buchovecky CM, Turley SD, Brown HM, *et al.* A suppressor screen in Mecp2 mutant mice implicates cholesterol metabolism in Rett syndrome. *Nat Genet* 2013; **45**:1013-1020.
29 Ricceri L, De Filippis B, Fuso A, Laviola G. Cholinergic hypofunction in MeCP2-308 mice: beneficial neurobehavioural effects of neonatal choline supplementation. *Behav Brain Res* 2011; **221**:623-629.
30 Kerr B, Alvarez-Saavedra M, Saez MA, Saona A, Young JI. Defective body-weight regulation, motor control and abnormal social interactions in Mecp2 hypomorphic mice. *Hum Mol Genet* 2008; **17**:1707-1717.
31 Pintaudi M, Calevo MG, Vignoli A, *et al.* Epilepsy in Rett syndrome: Clinical and genetic features. *Epilepsy Behav* 2010; **19**:296-300.

32 Picciotto MR, Higley MJ, Mineur YS. Acetylcholine as a neuromodulator: Cholinergic signaling shapes nervous system function and behavior. *Neuron* 2012; **76**:116-129.
33 Vallejo YF, Buisson B, Bertrand D, Green WN. Chronic nicotine exposure upregulates nicotinic receptors by a novel mechanism. *J Neurosci* 2005; **25**:5563-5572.
34 Sallette J, Pons S, Devillers-Thiery A, *et al.* Nicotine upregulates its own receptors through enhanced intracellular maturation. *Neuron* 2005; **46**:595-607.
35 Kawai H, Zago W, Berg DK. Nicotinic alpha 7 receptor clusters on hippocampal GABAergic neurons: Regulation by synaptic activity and neurotrophins. *J Neurosci* 2002; **22**:7903-7912.
36 Pidoplichko VI, Prager EM, Aroniadou-Anderjaska V, Braga MF. alpha7-Containing nicotinic acetylcholine receptors on interneurons of the basolateral amygdala and their role in the regulation of the network excitability. *J Neurosci* 2013; **110**:2358-2369.
37 Nag N, Mellott TJ, Berger-Sweeney JE. Effects of postnatal dietary choline supplementation on motor regional brain volume and growth factor expression in a mouse model of Rett syndrome. *Brain Res* 2008; **1237**:101-109.
38 Vega-Flores G, Rubio SE, Jurado-Parras MT, *et al.* The GABAergic septohippocampal pathway is directly involved in internal processes related to operant reward learning. *Cereb Cortex* 2014; **24**:2093-2107.
39 Roland JJ, Stewart AL, Janke KL, *et al.* Medial Septum-Diagonal Band of Broca (MSDB) GABAergic regulation of hippocampal acetylcholine efflux is dependent on cognitive demands. *J Neurosci* 2014; **34**:506-514.
40 Karvat G, Kimchi T. Acetylcholine elevation relieves cognitive rigidity and social deficiency in a mouse model of autism. *Neuropsychopharmacology* 2014; **39**:831-840.
41 Aliane V, Perez S, Bohren Y, Deniau JM, Kemel ML. Key role of striatal cholinergic interneurons in processes leading to arrest of motor stereotypes. *Brain* 2011; **134**:110-118.
42 Zaborszkey L, Duque A. Local synaptic connection of basal forebrain neurons. *Behav Brain Res* 2000; **115**:143-158.
43 Xu M, Chung S, Zhang S, *et al.* Basal forebrain circuit for sleep-wake control. *Nat Neurosci* 2015; **18**:1641-7.
44 Nicoll RA. The septohippocampal projection: A model cholinergic pathway. *Trends Neurosci* 1985; **8**:533-536.
45 Son JH, Winzer-Serhan UH. Expression of neuronal nicotinic acetylcholine receptor subunit mRNAs in rat hippocampal GABAergic interneurons. *J Comp Neurol* 2008; **511**:286-299.
46 Goldberg EM, Clark B D, Zagha E, *et al.* K^+ channels at the axon initial segment dampen near-threshold excitability of neocortical fast-spiking GABAergic interneurons. *Neuron* 2008; **58**:387-400.
47 Chahrour M, Jung SY, Shaw C, *et al.* MeCP2, a key contributor to neurological disease, activates and represses transcription. *Science* 2008; **320**:1224-1229.
48 Yasui DH, Scoles HA, Horikes S, *et al.* 15q11.2-13.3 chromatin analysis reveals epigenetic regulation of CHRNA7 with deficiencies in Rett and autism brain. *Hum Mol Genet* 2011; **20**:4311-4323.

(**Supplementary information** is linked to the online version of the paper on the *Cell Research* website.)